

Article

Numerical Analysis of the CIRCE-HERO PLOFA Scenarios

Moscardini Marigrazia ^{1,*}, Galleni Francesco ¹, Pucciarelli Andrea ¹ , Martelli Daniele ² and Forgiione Nicola ¹

¹ Department of Civil and Industrial Engineering, University of Pisa, 56122 Pisa, Italy; francescog.galleni@dici.unipi.it (G.F.); andrea.pucciarelli@dici.unipi.it (P.A.); nicola.forgione@unipi.it (F.N.)

² ENEA, FSN-ING, Brasimone Research Centre, 40032 Camugnano (Bo), Italy; daniele.martelli@enea.it

* Correspondence: marigrazia.moscardini@dici.unipi.it

Received: 7 September 2020; Accepted: 16 October 2020; Published: 21 October 2020



Abstract: The present work deals with simulations carried out at the University of Pisa by using the System Thermal Hydraulics code RELAP5/Mod3.3 to support the experimental campaign conducted at the ENEA (Energia Nucleare ed Energie Alternative) Brasimone Research Centre on the CIRColazione Eutettico—Heavy liquid metal pressurized water cooled tubes (CIRCE-HERO) facility. CIRCE is an integral effect pool type facility dedicated to the study of innovative nuclear systems and cooled by heavy liquid metal, while HERO is a heat exchanger heavy liquid metal/pressurized cooling water system hosted inside the CIRCE facility. Beside the H2020 project Multi-Purpose Hybrid Research Reactor for High-Tech Applications (MYRRHA) Research and Transmutation Endeavour (MYRTE), a series of experiments were performed with the CIRCE-HERO facility, for both nominal steady-state settings and accidental scenarios. In this framework, the RELAP5/Mod3.3 code was used to simulate the experimental tests assessing the heat losses of the facility and analyzing the thermal hydraulics phenomena occurring during the postulated Protected Loss Of Flow Accident (PLOFA). The modified version Mod. 3.3 of the source code RELAP5 was developed by the University of Pisa to include the updated thermo-physical properties and convective heat transfer correlations suitable for heavy liquid metals. After reproducing the facility through an accurate nodalization, boundary conditions were applied according to the experiments. Then, the PLOFA scenarios were reproduced by implementing the information obtained by the experimental campaign. Sensitivity analyses of the main parameters affecting the thermofluidynamics of the Lead-Bismuth Eutectic (LBE) were carried out. In the simulated scenario, the LBE mass flow rate strongly depends on the injected argon flow time trend. The numerical results are in agreement with the experimental data, however further investigations are planned to analyze the complex phenomena involved.

Keywords: LBE; PLOFA; CIRCE-HERO; RELAP5/Mod3.3; thermohydraulics

1. Introduction

The Lead-Cooled Fast Reactor (LFR) is one of the six nuclear reactor concepts selected by the Generation IV International Forum (GIF) to sustain the R&D of the next generation of nuclear energy systems [1]. The LFRs are cooled by Heavy Liquid Metals (HLM) such as lead or Lead-Bismuth Eutectic (LBE), employing a fast-neutron spectrum and a closed fuel cycle for efficient conversion of fertile uranium and management of actinides. The main advantages of using HLMs as coolant are [2]:

- high thermal inertia;
- very low absorption and scattering cross sections;
- high boiling points allowing a low-pressure operation;

- good natural circulation due to the high density.

Compared to sodium, lead and LBE has the key advantage of being an inert coolant without exhibiting violent chemical reactions with air and water. Therefore, by using lead or LBE the steam generator is located inside the reactor vessel, generating an integral compact system with the core and the coolant pump. As a shortcoming, lead and LBE are both weaker absorbers and moderators than sodium, allowing a larger amount of coolant in the core, forming wider cross sections of the flow paths and thus increasing the thermal inertia of the pool. Furthermore, the coolant is characterized by relatively low velocities which are necessary to mitigate the structural erosion. As a consequence, the pressure drops are reduced and the natural circulation is improved. Compared to lead, the advantage of LBE is the decreased freezing risk determined by lower melting temperature [1–4].

Unfortunately, operational experience of LFRs is limited and further investigation is required to provide a larger amount of information regarding several aspects of the HLM systems. In particular, both the thermal–hydraulic behavior during normal operation and the scenarios generated by severe accident are key points for the designers. Besides the necessity of experimental campaigns, numerical analyses are strongly required to investigate the thermal–hydraulic aspects of HLMs. In this framework, the two projects thermal–hydraulics Simulations and Experiments for the Safety Assessment of MEtal cooled reactors (SESAME) and MYRRHA Research and Transmutation Endeavour (MYRTE) of HORIZON 2020, were launched. SESAME project was established to support the development of European liquid metal fast reactors, while the MYRTE project aims at studying the transmutation of high-level waste at industrial scale through the development of the Multi-Purpose Hybrid Research Reactor for High-Tech Applications (MYRRHA) research facility [3]. Inside these two projects, both experimental campaigns and numerical analyses were planned. Among the available numerical tools, the System Thermal Hydraulic (STH) codes are the most used because of their solid background.

In the present work the STH code RELAP5/Mod3.3 [5,6] was used to support the experimental campaign conducted at the ENEA (Energia Nucleare ed Energie Alternative) Brasimone Research Centre on the CIRColazione Eutettico- Heavy liquid mEtal pRessurized water cOoled tubes (CIRCE-HERO) facility [7,8]. The version of RELAP5/Mod3.3 employed for this purpose was modified at Laboratory of Numerical Simulation for Nuclear Thermohydraulics of the University of Pisa by including the thermodynamic properties of lead and LBE, adding the updated transport properties for viscosity, thermal conductivity, surface tension and specific convective heat transfer correlations for liquid metals [9]. In particular, the thermodynamic properties of LBE were implemented according to the Sobolev's work [10], while heat transfer correlations developed for liquid metals by Ushakov [11] and Seban-Shimazaki [12] were implemented as well. Lacking the physic and specific correlations for transported incondensable gases in liquid metals, the tables and flow regime maps developed for water and already implemented in the code were assumed as a good first approximation. In recent years, several works have been carried out to assess, validate and improve this code version [13–19]. The numerical activity performed in this work is focused on the analysis of the Protected Loss of Flow Accident (PLOFA) test carried out in CIRCE-HERO [8]. Afterwards, sensitivity analyses of the main parameters affecting the thermo–fluid-dynamics of the Lead-Bismuth Eutectic (LBE) were carried out.

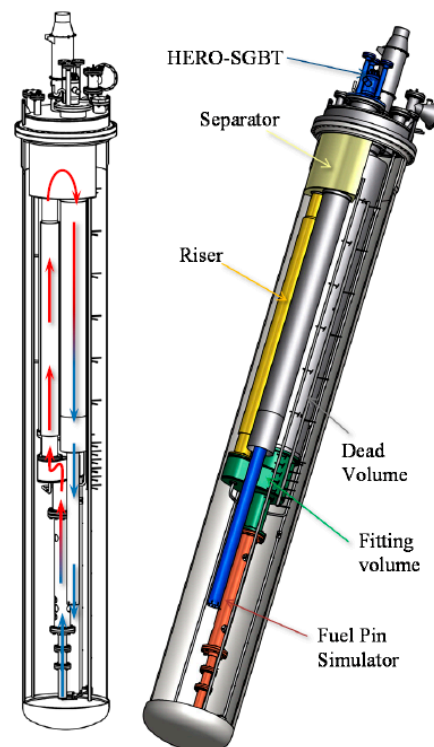
2. Experimental Facility

CIRCE is an integral effect pool-type facility, designed and constructed at the ENEA Brasimone research center. It consists of a cylindrical main vessel of AISI316L partially filled with nearly 70 tons of molten LBE covered with argon at about 0.2 bar [7,8]. The vessel is externally equipped with electrical heating cables installed at the bottom and on the lateral surface and operating in a temperature range of 200 °C–400 °C. The pool vessel parameters are summarized in Table 1. The HERO-loop test section is installed inside CIRCE from the top of the main vessel through a coupling flange; a schematic view of the CIRCE-HERO facility is reported in Figure 1.

Table 1. Pool vessel parameters.

CIRCE Parameters	Value
Outside diameter [mm]	1200
Hight [mm]	8500
Wall thickness [mm]	15
Electrical heating [kW]	47
Operating pressure [kPa]	15 (gauge)
Design pressure [kPa]	450 (gauge)
Argon gas volumetric flow rate [Nl/s]	5

CIRCE: CIRColazione Eutettico—Heavy liquid mEtal pResurized water cOoled tubes.

**Figure 1.** Schematic view of the CIRCE-HERO facility.

The HERO-loop consists of:

- A Fuel Pin Simulator (FPS), an electrical pin bundle composed of 37 electrically heated pins with a nominal thermal power of ~ 1 MW representing the heat source of the LBE. The design of the component aims to provide a coolant temperature gradient of 100 °C/m with an LBE average speed of 1 m/s and a power density of 500 W/cm³.
- A fitting volume, a volume located above the FPS collecting the hot LBE rising from the FPS.
- A riser, in which the LBE flows upward up to the separator.
- A separator, a component sited on the top of the test section. It is the hot plenum and acts as an expansion tank accommodating the LBE volume variations.
- A Steam Generator Bayonet Tube (SGBT), the heat sink of the loop for heat removal. It is composed of 7 double wall bayonet tubes. Each tube represents in scale 1:1 the tube foreseen for the SGBT to be adopted in the Advanced Lead Fast Reactor European Demonstrator-super (ALFRED) [7]. This configuration guarantees the separation between the primary side (LBE) and the secondary side (steam-water) decreasing the probability of LBE-water interaction and facilitating the monitoring of leakages by pressurizing the annular separation region.

- An argon injection device is located at the inlet section of the riser. It circulates the LBE by imposing a fixed argon mass flow rate.
- A dead volume, placed above the fitting volume and insulated from the pool, which encloses and maintains the wirings and electrical connections of the FPS.

A feeding conduit equipped with an LBE Venturi flow meter and a differential pressure transmitter allows the measuring of the LBE flowing upwards through the FPS region where it is heated up by the 37 electrical pins. Then the LBE passes through the fitting volume and the riser (at this point the flow is enhanced by the argon gas injection at the top of the fitting volume) reaching the separator. From the separator, the LBE enters the shell side (primary side) of the HERO-SGBT flowing downwards. Here, the LBE is cooled by the feedwater flowing in the 7 Bayonet Tubes (BTs) (1 central tube and 6 lateral tubes allocated in a hexagonal arrangement) to then be discharged in the bottom zone of the pool. Further details regarding the facility are reported in [7,8].

3. PLOFA Test

The test aims at analyzing the mixed convection and thermal stratification phenomena that take place into a pool filled with heavy liquid metal during the transition from forced convection (nominal conditions) to natural circulation (accidental scenario). The experiment involves a PLOFA scenario where a sudden degradation in the heat transfer capability occurs due to a sharp decrease in the flow rate. The test described in this work was selected to represent the reference test for the benchmark calculations of SESAME project. The test starts when the steady-state condition is approximately reached with an FPS power of 356 kW and forced circulation condition in the HERO-loop. The forced circulation of the LBE was provided by buoyancy effects and enhanced by argon gas injection. During the initial stage of the experiment, the argon flow rate was 2.75 Nl/s and the resulting LBE mass flow rate was about 34 Kg/s. Inside HERO SGBT the heat was removed by means of water flowing in the secondary side with a total mass flow rate of 0.264 Kg/s, an inlet temperature of about 336 °C and pressure equal to 175 bar. The transient was triggered after about half an hour, and the FPS power was reduced to a value of about 20 kW according to the curve shown in Figure 2.

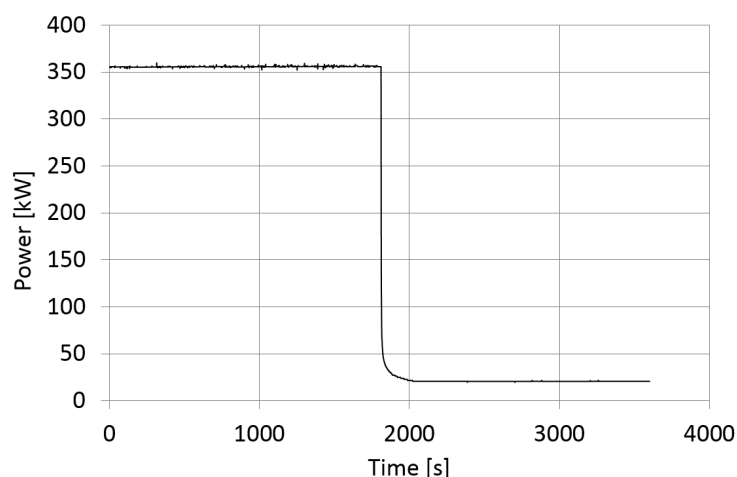


Figure 2. Fuel Pin Simulator (FPS) electrical power time trend.

The gas injection was decreased sharply from 2.75 Nl/s to 0 generating the corresponding LBE mass flow rate shown in Figure 3. After the transient, the LBE flow was induced only by the natural circulation in the loop and was oscillating around a value of 6 Kg/s. The feedwater was reduced to 30% of the steady-state value in a time ramp of 2 s as reported in Figure 4.

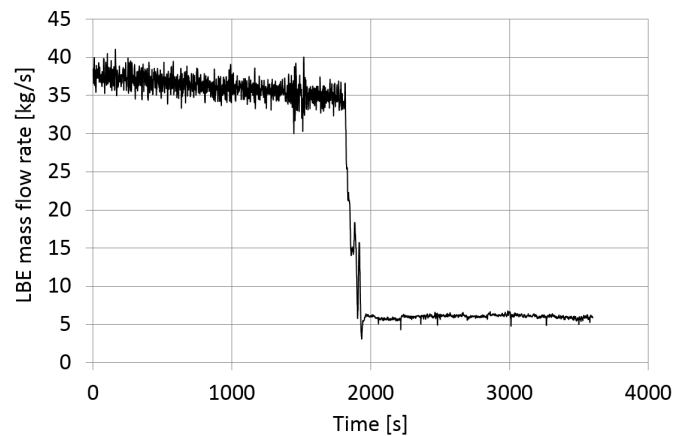


Figure 3. Lead-Bismuth Eutectic (LBE) mass flow rate time trend.

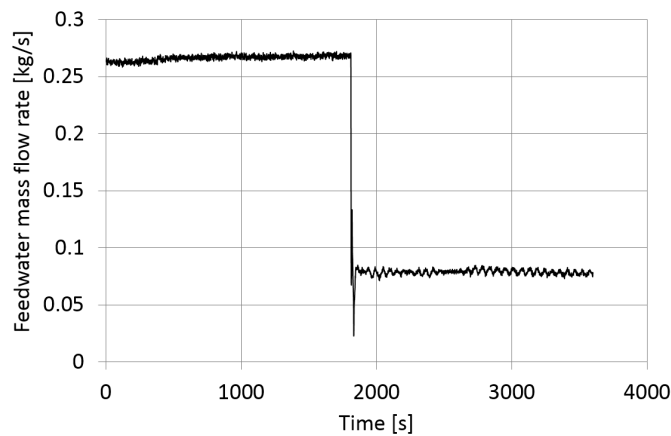


Figure 4. Feedwater mass flow rate time trend.

4. RELAP5/Mod.3.3 Nodalization

The RELAP5 nodalization of the CIRCE-HERO facility is Figure 5. It is worth mentioning the presence of RELAP5 default structures called ANNULUS—used in this case to simulate the steam generator components—which are similar to pipes, but require that all the water must be in a film on the wall (no drops) in the annular mist flow regime (ANNULUS structure [5,6]). Details concerning the implemented components are reported in the Appendix A. The nodalization of the HERO-loop is designed according to the following configuration:

- The feeding conduit is modelled with PIPE 20 which is connected to the downstream mixing zone of the FPS (PIPE 50) by means of a Single Junction, (SNGLJUN [5,6]).
- The FPS region is modelled with PIPES 50, 60, and 70 where the active length of the FPS (1000 mm active region) is modelled with PIPE 60. The FPS is modelled using a heat structure inside the pipe 60 with a source term representing the power generated by the 37 electrical pins. The upstream mixing zone of the FPS (PIPE 70) is connected to the fitting volume.
- The fitting volume is represented via PIPE 80 and BRANCH 90 [5,6] and it is connected to the riser by means of a SNGLJUN.
- At the inlet of the riser (PIPE 130) argon gas is injected to enhance the LBE circulation. This argon injection system is modelled with Time Dependent Volume 3, (TMDPVOL [5,6]).
- After the riser, the separator is modelled by BRANCH 132. Furthermore, it is connected to the argon cover gas volume (TMDPVOL 151) through the BRANCH 150.
- Connected to the separator there is the PIPE 172 which represents the primary side (LBE side) of the SGBT. LBE is released into the pool by means of PIPE 174.

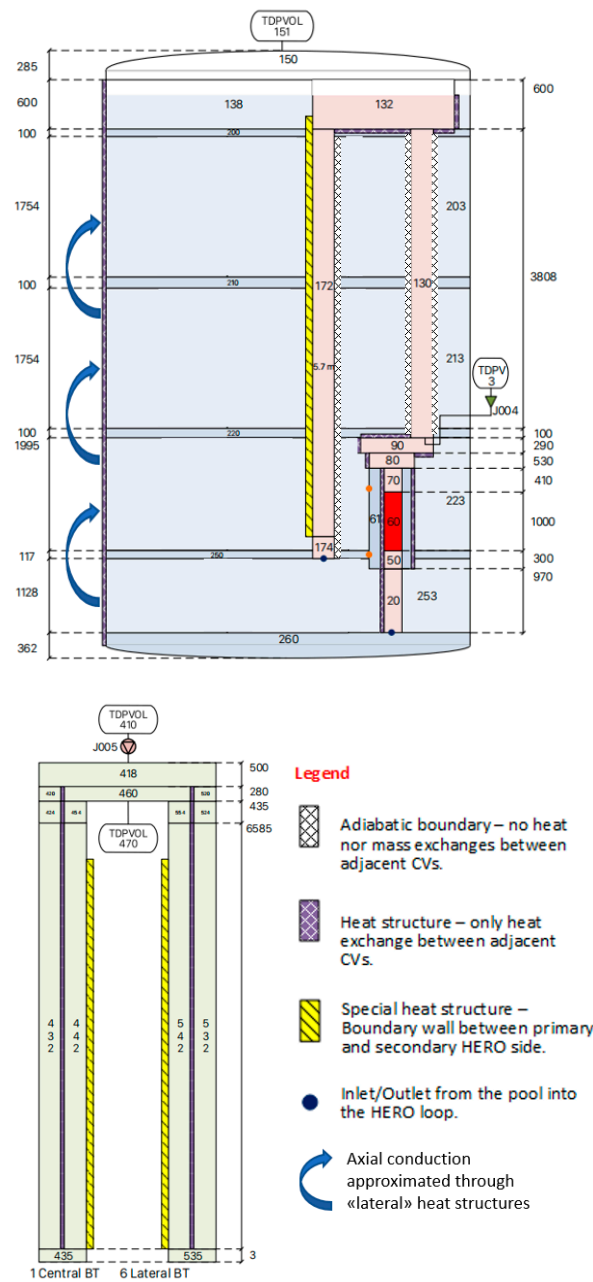


Figure 5. Nodalization of CIRColazione Eutettico—Heavy liquid mEtal pRessurized water cOoled tubes (CIRCE-HERO).

The primary side of the SGBT is connected to the secondary side (steam-water) by means of a heat structure. The secondary side is modelled as follow:

- The feedwater manifold is modelled with TMDPVOL 410.
- The feedwater flow rate is supplied to the system via the TMDPJUN (Time Dependent Junction, [5,6]) connecting TMDPVOL 410 to the BRANCH 418, which models the feedwater inlet header to the BTs.
- The central BT (PIPES 432, 420 and 424 for the feedwater inlet, and ANNULUS 442, and 454 for the steam outlet).
- The 6 lateral BTs (PIPES 532, 520 and 524 for the feedwater inlet, and ANNULUS 542 and 554 for the steam outlet).
- The outlet steam plenum (BRANCH 460) connected to the steam chamber (TMDPVOL 470).

The pool is modelled via a group of pipes, i.e., PIPES 203, 213, 223 and 253. These pipes are vertically connected via branches, i.e., BRANCHES 200, 210, 220, 250. The upper and the lower plenum are modelled by means of BRANCHES 150 and 260, respectively. The upper plenum is connected to BRANCH 200 through BRANCH 138. The lower plenum is connected to the feeding circuit of the HERO-loop through a SNGLJUN.

Concerning the heat structures, the active length of the FPS region is modelled as a power source embedded inside the thermal structure of PIPE 60. The power source is defined by a power time trend card and the Ushakov heat transfer correlation [10] is used for the triangular lattice fuel bundle region. Furthermore, the following heat structures and wall boundary conditions were applied:

- Heat structures between the primary and the secondary side of the BTs of the SGBT. Both ANNULUS 442 (central BT) and ANNULUS 542 (6 lateral BTs) are connected to PIPE 172. This heat structures model the heat transfer between LBE and steam-water flowing inside BTs.
- Heat structure in the secondary side of the central BT, which is connected from one side to the water (pipe 432), and the other side to steam (ANNULUS 442). As well as for the 6 lateral BTs the heat structure links the water side PIPE 532 to the steam ANNULUS 542. Similar heat structures are used to connect BRANCH 460 to PIPES 420, 520 and to link PIPE 424 and PIPE 524 to ANNULUS 454 and 554, respectively.
- Adiabatic conditions are applied between the pool and the external environment as well as between the pool and PIPES 172 and 130.
- Heat structures were applied between the pool and the HERO-loop (from PIPE 20 to BRANCH 90).
- In order to simulate the axial thermal conduction inside the pool, heat structures were applied according to the arrows reported in Figure 5 and connecting PIPES 203-213, 213-223, 223-253 and PIPE 253 with BRANCH 260.

5. Results and Discussions

In this section, the numerical results obtained by using the nodalization described in Section 3 and applying the boundary conditions of the experimental test reported in Section 2 are presented. According to the boundary conditions of the experimental test, a transient of 3600 s was simulated by imposing the PLOFA starting time at 1800 s. The FPS power was imposed according to Figure 2.

Similarly to the experiment, the required LBE mass flow rate is obtained by imposing the Argon mass flow rate (TDPV3 and J004 in Figure 5), as explained in Section 2. In Figure 6 the experimental LBE mass flow rate is reported with black diamonds, while the numerical value obtained by applying the nominal conditions is reported with a dotted light blue line. Due to the approximation introduced by the simplified numerical geometry and the assumptions adopted in terms of concentrated pressure drops, the obtained LBE mass flow rate overestimates the experimental value. Therefore, in order to assure the same initial conditions of the experiments, the LBE mass flow was reduced by following two different approaches. As a first approach, the pressure drops inside the riser (PIPE 130) were increased, the resulting LBE mass flow is reported with the dash-dotted orange line. As a second approach, the LBE mass flow was directly imposed as an input parameter according to the dashed purple line shown in Figure 6. In these simulations, mass flow rates are applied by using the component TMDPJUN, which joins a TMDPVOL to the corresponding hydrodynamic volume. The TMDPVOL imposes the desired temperature, pressure and static quality of the injected fluid, while the TMDPJUN applies the chosen mass flow rate (liquid and/or gas phase) as a function of the time. Thus, under both forced circulation during normal operation and natural circulation after the PLOFA, the thermal behavior of the system is simulated. The initial temperature of both the whole HERO-loop and the bottom part of the pool (PIPE 253–BRANCH 260) was set to 420 °C. According to the experiment, a temperature equal to 475 °C was initially applied in the rest of the pool [7,8]. For the secondary side of the SGBT the inlet temperature of the water was set equal to 336 °C and the related mass flow rate was implemented according to Figure 4.

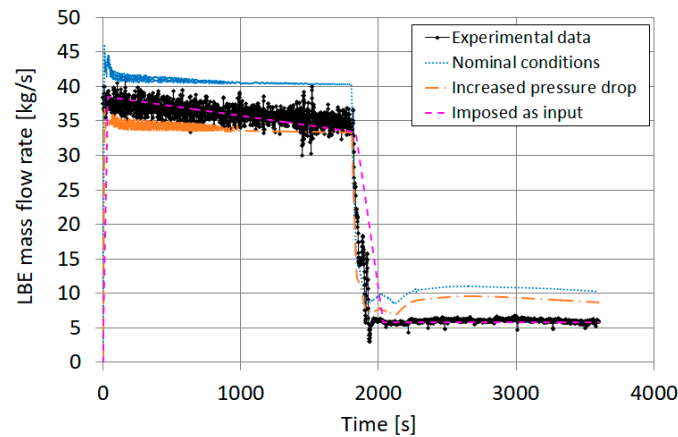


Figure 6. LBE mass flow rate. Comparison between experimental data and numerical results obtained under different conditions.

In this work results in terms of the temperatures reached inside the FPS and in the outlet region of HERO-SGBT are also reported and analyzed. In Figure 7 the temperature trends measured during the experiment at the inlet and outlet of the FPS are reported and compared to the related numerical values obtained by implementing the different trends of LBE mass flow rate reported in Figure 6. In the same way, Figure 8 shows the comparison between experimental and numerical results of the HERO-SGBT outlet temperature. In the legends of both Figures 7 and 8 the experimental data are nominated with “Exp.,” the numerical analysis carried out under nominal condition with “Nom.,” while numerical cases with increased pressure drops and LBE mass flow rate imposed as input are reported with “PressDrop” and “ImpInp”, respectively.

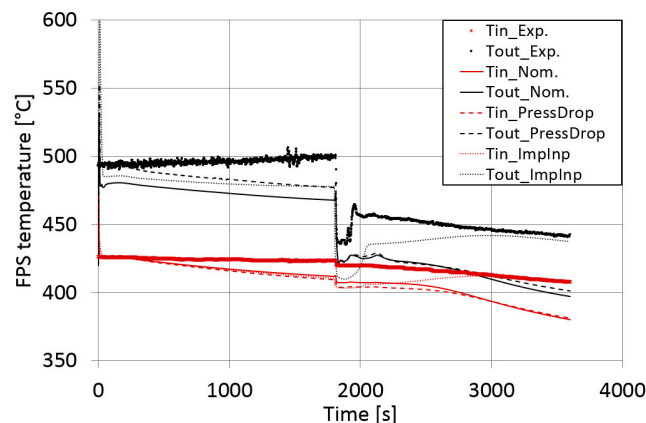


Figure 7. FPS inlet and outlet temperatures. Comparison between experimental data and numerical results obtained under different conditions.

According to the obtained numerical results, by approaching the experimental LBE mass flow rate the FPS temperatures evaluated numerically become closer to the related experimental results. Before the PLOFA starting time, the inlet and outlet temperature slightly increase in the experiments while both decrease in the numerical analyses. Furthermore, compared to the nominal case, when a lower LBE mass flow rate is applied a more effective cooling is performed by the water mass flow rate, which is kept constant. As a result, a lower LBE temperature is evaluated. After the transient, the experimental and numerical analyses behave similarly from a qualitative point of view for: both the nominal case and the numerical analysis with increased pressure drops in the riser. The temperature decreases in both cases, however, a difference of about 10% is found at the end of the simulation between experimental and numerical results. On the contrary, the third numerical analysis, named ‘ImpInp’, generates a temperature increase after the PLOFA, converging to the FPS temperature of the experiment,

with a difference of about 0.1% at the end of the simulation. This behavior is determined by the increase in the temperature at the HERO-loop outlet (see Figure 7) due to the combination “LBE mass flow rate—FPS power” occurring soon after the PLOFA. Indeed, LBE mass flow rate decreases up to 6 Kg/s according to the experiments, while in the other two simulations the value stays around 10 Kg/s. Under this condition, the FPS power (20 kW) easily warms up the LBE increasing the temperature at the HERO-loop outlet and as a consequence at the FPS inlet. In all cases, the differences occurring before the PLOFA starting time could be due to the continuous reduction of the FPS inlet temperature, which should be instead almost constant. This reduction is generated by the same temperature reduction of the LBE at the outlet of HERO-SGBT (see Figure 8). This entails that when LBE comes out the SGBT it enters almost directly into the FPS maintaining the same temperature. Looking at the CFD (Computational Fluid Dynamics) results reported in the literature [17], a longer and more complex path is made by LBE from the outlet of HERO-SGBT to the inlet of the FPS. Indeed, according to [17], soon after entering in the pool, the LBE hits the lower plenum rising the pool in the opposite direction up to the outlet zone of the SGBT to then conclude the path flowing down to the inlet of the FPS. During this route, the LBE has more time to warm up, keeping its FPS inlet temperature almost constant at 420 °C. Therefore, as a further study, the volume of the lower plenum was intentionally increased by one order of magnitude to let the LBE warm sufficiently.

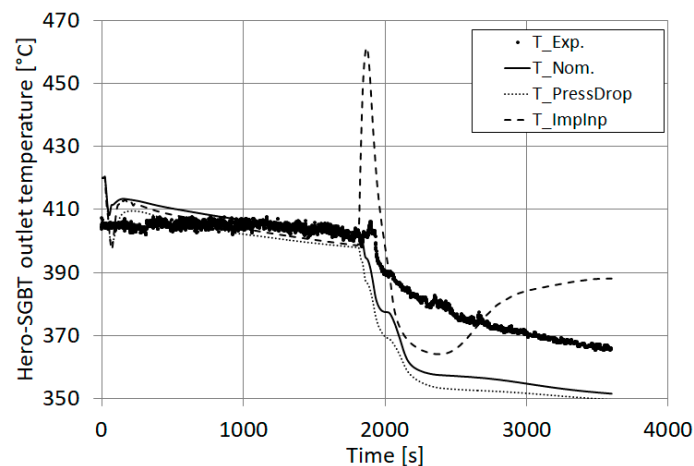


Figure 8. HERO- Steam Generator Bayonet Tube (SGBT) outlet temperatures. Comparison between experimental values and numerical results obtained under different conditions.

After the PLOFA, the low LBE mass flow could generate a different flow path, avoiding LBE hitting the lower plenum after leaving the HERO-loop and flowing directly to the inlet of the FPS. This behavior joined to the applied combination “LBE mass flow rate- FPS power”, which determines the same temperature at the end of the simulation.

Figure 9 shows the comparison between the experimental FPS temperatures and the related numerical values obtained by increasing the volume of the pool lower plenum. Here, the case with LBE mass flow rate imposed as input parameter was considered. A good agreement between numerical and experimental results during the entire analysis is obtained for both quantitative and qualitative study. This reveals the importance of a coupled CFD-STH analysis to include the exact path made by the LBE and evaluate the resulting temperature. While FPS experimental temperature decreases after PLOFA, numerical results remain almost constant, generating a temperature difference of about 3% at 3600 s. This behavior is generated by the approximation introduced by increasing the volume of the lower plenum. Figure 10 shows the variation of the temperature trend generated in the lower plenum by increasing its volume by one order of magnitude starting from about 1 m³. When the volume increases the temperature remains almost constant generating a different outlet temperature in the FPS.

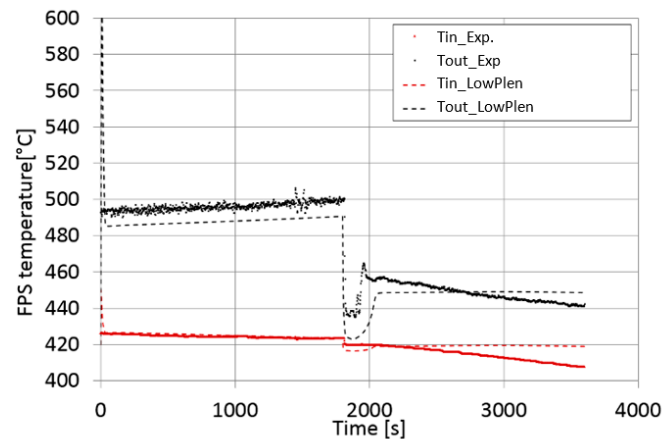


Figure 9. FPS inlet and outlet temperatures. Comparison between experimental and numerical results obtained by increasing the volume of the lower plenum.

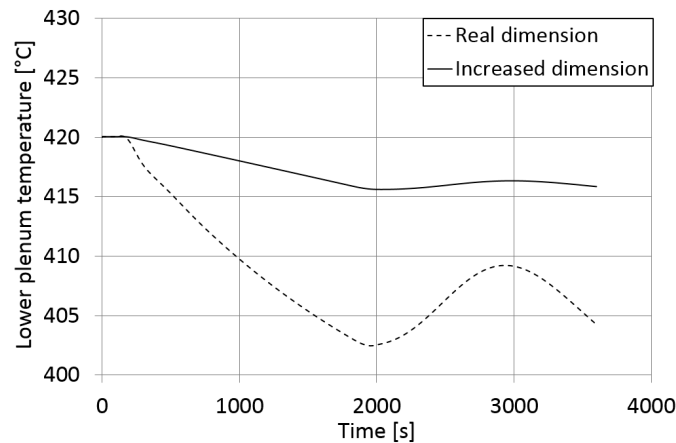


Figure 10. Lower plenum temperatures. Comparison between numerical results obtained by simulating the lower plenum with the increased volume and real size.

The facility represents a complicated thermal–hydraulic system which involves two-phase flow, non-condensable gas and liquid metal flow conditions. In this framework, a stand-alone approach could not be sufficient for addressing all the involved phenomena, while a coupled CFD-STH application may represent the best option to obtain a suitable representation of the thermo–hydraulic behavior of this system. Thus, further CFD-STH coupled analyses were recently performed obtaining promising results in predicting the observed phenomena, details are reported in [19].

6. Conclusions

This work aimed at evaluating the phenomena occurring in HLM pool-type systems as a result of a Protected Loss Of Flow Accident (PLOFA) by using the last updated version of the STH code RELAP5/mod3.3 made by the University of Pisa (UNIPI) to take into account liquid metals as working fluids.

For this purpose, an experimental campaign launched in the framework of different projects involved in HORIZON 2020 was considered. The numerical analyses were performed at UNIPI, while the experimental campaign was carried out at the ENEA Brasimone Research Centre.

The CIRCE-HERO test facility was simulated through a full detailed model by adopting the most convenient nodalization. Standalone simulations were performed to simulate the PLOFA scenario by setting up appropriate boundary conditions to reproduce the experimental trends. The PLOFA scenario is characterized by a sudden degradation in the heat transfer capability due to the sharp decrease in the

feedwater flow, accompanied by the transition from forced circulation (nominal conditions) to natural circulation. The STH analyses show a quantitative agreement between numerical and experimental results in terms of temperature reached inside the HERO-loop. However, numerical results differ qualitatively from the experimental values especially before the PLOFA transient.

The authors judge these discrepancies a consequence of the difficulty of simulating the real path of the LBE when it is released inside the pool. Therefore, a coupled CFD-STH analysis is strongly required to detect the right route of the fluid in the pool and thus to determine the correct temperature reached in the LBE.

Author Contributions: Investigation and Formal Analysis; M.M.; writing original draft, writing, reviewing and editing; M.M., G.F., P.A., F.N., M.D.; project administration and supervision; F.N. All authors have read and agreed to the published version of the manuscript.

Funding: This work was performed in the framework of the H2020 SESAME project. This project has received funding from the Euratom research and training program 2014.2018 under grant agreement No 654935.

Conflicts of Interest: The authors declare no conflict of interest.

Appendix A

In this appendix a dedicated description of the main components used to perform the RELAP5/Mod3.3 nodalization of CIRCE-HERO facility is reported. It consists of hydrodynamic volumes and heat structures. The hydrodynamic volumes include the following components:

1. Time-dependent volume (TMDPVOL) is a hydrodynamic boundary volume used to specify a fluid state boundary condition. Quantities such as pressure, liquid temperature, vapour temperature, void fraction, and quality can be set as boundary conditions. The TMDPVOL provides the user with a mechanism for absolutely defining the fluid condition at a point in the model. The user should consider that a TMDPVOL acts as an infinite fluid source or sink. Its conditions remain unchanged (or vary) as requested, but are invariant with inflow or outflow [5,6].
2. A Time-dependent junction (TMDPJUN) component allows the user to impose a flow boundary condition on a model. It is possible to specify the flow condition as either a volumetric or mass flow rate. An example of this capability is the specification of an injection flow as a function of the coolant system pressure. TMDPJUN capabilities include varying the flow condition in any manner and as a function of any problem variable the user desires [5,6].
3. A Single-Volume component (SNGLVOL) is the basic hydrodynamic cell unit. The flow area, length, and volume of the cell must be defined by the user to describe the geometry in the input file. The input flow area determines the flow velocity, the input length affects the calculated frictional pressure drop, and the input volume contributes to the overall fluid system volume [5,6].
4. A Single-Junction component (SNGLJUN) is the basic hydrodynamic flow unit. Each junction is used to connect hydrodynamic volumes, which are characterized by an inlet and outlet face [5,6].
5. A Pipe (PIPE) component is a hydrodynamic volume component. As a function of the length it can be set as series combination of single-volumes joined by single-junctions. The advantage of the pipe over the separate single components is primarily one of input efficiency, reducing significantly the number of data cards to include. By definition, the pipe component has only internal junctions associated with it. Any connections to the ends of a pipe must be made with external junctions. Furthermore, it is possible to connect external junctions to any face of internal pipe cells and any face of pipe cells at the ends of a pipe [5,6].
6. An Annulus component (ANNULUS) is identical to the pipe component except that an annular flow regime map is used. An annulus must be specified as a vertical component [5,6].
7. A Branch component (BRANCH) is a single-volume component that may have single-junctions appended [X].

The heat structures are used to represent metal structures such as vessel walls, steam generator tubes, fuel rods, and reactor vessel internals in a facility. Each heat structure is defined to connect

thermally a “left” and a “right” side. Each side of a heat structure may be connected to at most one hydrodynamic volume. However, more than one heat structure may be connected to the same hydrodynamic volume. The geometry of the heat structure can be chosen as well as the desired boundary condition (surface temperature or surface heat flux). Adiabatic, conductive and convective boundary conditions can be activated. The default convection and boiling correlations were derived mainly based on data from internal vertical pipe flow [5,6].

References

1. Baudrand, O.; Blanc, D.; Bourgois, T.; Ivanov, E.; Bonneville, H.; Bruna, G.; Clément, B.; Hache, G.; Kissane, M.; Meignen, R.; et al. *Overview of Generation IV (Gen IV) Reactor Designs-Safety and Radiological Protection Considerations*; IRSN Rep. 2012/158; Institut de Radioprotection et de Sureté Nucleaire-IRSN: Fontenay-aux-Roses, France, 2012; Volume 44.
2. Roelofs, F. *Thermal Hydraulics Aspects of Liquid Metal Cooled Nuclear Reactors*; Woodhead Publishing; Elsevier: Duxford, UK, 2019.
3. Alemberti, A.; Smirnov, V.; Smith, C.F.; Takahashi, M. Overview of lead-cooled fast reactor activities. *Prog. Nucl. Energy* **2014**, *77*, 300–307. [[CrossRef](#)]
4. “GIF 2019 Annual Report”, Generation IV International Forum. 2019. Available online: https://www.gen-4.org/gif/jcms/c_119034/gif-2019-annual-report (accessed on 13 October 2020).
5. Fletcher, C.D.; Schultz, R.R. *RELAP5/Mod3.3 Code Manual Volume I: Code Structure, System Models, and Solution Methods*; Nuclear Safety Analysis Division; Information Systems Laboratories, Inc.: Rockville, MD, USA; Idaho Falls, ID, USA, 2001.
6. Fletcher, C.D.; Schultz, R.R. *RELAP5/Mod3.3 Code Manual Volume V: User’s Guidelines*; Nuclear Safety Analysis Division; Information Systems Laboratories, Inc.: Rockville, MD, USA; Idaho Falls, ID, USA, 2001.
7. Lorusso, M.; Pesetti, A.; Tarantino, M.; Narcisi, V.; Giannetti, F.; Forgione, N.; del Nevo, A. Experimental analysis of stationary and transient scenarios of alfred steam generator bayonet tube in circe-hero facility. *Nucl. Eng. Des.* **2019**, *352*, 110169. [[CrossRef](#)]
8. Lorusso, P.; Pesetti, A.; Barone, G.; Castelliti, D.; Caruso, G.; Forgione, N.; Giannetti, F.; Martelli, D.; Rozzia, D.; van Tichelen, K.; et al. MYRRHA primary heat exchanger experimental simulations on CIRCE-HERO. *Nucl. Eng. Des.* **2019**, *353*, 110270. [[CrossRef](#)]
9. Forgione, N.; Castelliti, D.; Gerschenfeld, A.; Polidori, M.; del Nevo, A.; Hu, R. System thermal hydraulics for liquid metals. In *Thermal Hydraulics Aspects of Liquid Metal Cooled Nuclear Reactors*; Roelofs, F., Ed.; Woodhead Publishing: Duxford, UK, 2019; pp. 157–184.
10. Sobolev, V. *Database of Thermophysical Properties of Liquid Metal Coolants for GEN-IV*; SCK•CEN Report BLG-1069; Centre D’etude de L’energie Nucléaire: Moll, Belgium, 2011; (rev. December 2011).
11. Ushakov, P.A.; Zhukov, A.V.; Matyukhin, N.M. Heat transfer to liquid metals in regular arrays of fuel elements TVT. *High Temp.* **1977**, *15*, 1027–1033.
12. Seban, R.A.; Shimazaki, T.T. Heat transfer to a fluid flowing turbulently in a smooth pipe with walls at constant temperature. *Trans. Am. Soc. Mech. Eng.* **1951**, *73*, 803–809.
13. Barone, G.; Martelli, D.; Forgione, N. Implementation of Lead-Lithium as working fluid in RELAP5/Mod3.3. *Fusion Eng. Des.* **2019**, *146*, 1308–1312. [[CrossRef](#)]
14. Forgione, N.; Angelucci, M.; Ulissi, C.; Martelli, D.; Barone, G.; Ciolini, R.; Tarantino, M. Application of RELAP5/Mod3.3-Fluent coupling codes to CIRCE-HERO. *J. Phys. Conf. Ser.* **2019**, *1224*, 012032. [[CrossRef](#)]
15. Forgione, N.; Martelli, D.; Barone, G.; Giannetti, F.; Lorusso, P.; Hollands, T.; Papukchiev, A.; Polidori, M.; Cervone, A.; di Piazza, I. Post-test simulations for the NACIE-UP benchmark by STH codes. *Nucl. Eng. Des.* **2019**, *353*, 110279. [[CrossRef](#)]
16. Forgione, N.; Angelucci, M.; Barone, G.; Polidori, M.; Cervone, A.; di Piazza, I.; Giannetti, F.; Lorusso, P.; Hollands, T.; Papukchiev, A. Blind simulations of NACIE-UP experimental tests by STH codes. In Proceedings of the International Conference on Nuclear Engineering, ICONE, 4, ASME, London, UK, 22–26 July 2018.
17. Gonfiotti, B.; Barone, G.; Angelucci, M.; Martelli, D.; Forgione, N.; del Nevo, A.; Tarantino, M. Thermal hydraulic analysis of the circe-hero pool-type facility. In Proceedings of the International Conference on Nuclear Engineering, ICONE, 6B, ASME, London, UK, 22–26 July 2018.

18. Buzzi, F.; Pucciarelli, A.; Galleni, F.; Tarantino, M.; Forgione, N. Analysis of the thermal stratification phenomena in the CIRCE-HERO facility. *Ann. Nucl. Energy* **2020**, *141*, 107320. [[CrossRef](#)]
19. Pucciarelli, A.; Galleni, F.; Moscardini, M.; Martelli, D.; Forgione, N. STH/CFD coupled simulation of the protected loss of flow accident in the CIRCE-HERO facility. *Appl. Sci.* **2020**, *10*, 7032. [[CrossRef](#)]

Publisher's Note: MDPI stays neutral with regard to jurisdictional claims in published maps and institutional affiliations.



© 2020 by the authors. Licensee MDPI, Basel, Switzerland. This article is an open access article distributed under the terms and conditions of the Creative Commons Attribution (CC BY) license (<http://creativecommons.org/licenses/by/4.0/>).